JOURNAL OF COMPUTATIONAL PHYSICS 74, 440–455 (1988)

Finite Element Analysis of Diffusion with Reaction at a Moving Boundary

PAUL MURRAY AND G. F. CAREY

TICOM, The University of Texas at Austin, Austin, Texas 78712

Received August 6, 1986; revised February 5, 1987

We consider the model problem of mass transport by diffusion with chemical reaction at a moving boundary. The objective is to model the chemical process by predicting the location of the boundary as the reaction proceeds in time. A finite element analysis is formulated in one dimension using moving elements to follow the boundary motion, and an iterative linearization method is developed to uncouple and solve the diffusion and reaction equations. The semidiscrete system for the transport process is integrated using a predictor–corrector scheme and its accuracy and stability are examined in numerical experiments. Numerical results are compared with an analytic solution for the quasi-steady case in which diffusion is very rapid in comparison to reaction and to a perturbation solution for the unsteady case. Other supporting numerical studies are made to examine the sensitivity of the solution and boundary motion to changes in diffusion and reaction rate for both linear and nonlinear reactions.

INTRODUCTION

Many chemical processes involve a reaction occurring at the interface between two phases (see Bird *et al.* [1]). An example is the oxidation of silicon used in semiconductor processing. A primary objective in engineering design studies is to predict the location of the interface, or moving boundary, as the reaction proceeds in time. In the example of combustion of a solid particle, it is desired to know the time required for the particle to react completely. Numerical simulation provides the most realistic approach to solving these types of problems due to their complexity: analytic solutions appear feasible only in one-dimensional and symmetric two-dimensional cases under certain assumptions on the relative rate of reaction as compared to diffusion (see Deal and Grove [4] for a discussion of silicon oxidation and Glassman [6] for application to coal combustion).

There are two important special cases of the general problem that need to be mentioned. One is the limiting case of an instantaneous reaction, described mathematically by the classical Stefan problem. There is an extensive literature on the Stefan problem for heat transport with phase change (see Cannon [2] and Friedman [5]). It should be emphasized that the mathematical structure of this

0021-9991/88 $3.00

problem is special because the reaction kinetics do not explicitly appear in the model, and is therefore usually distinguished from the more general problem involving kinetic rate boundary conditions considered here. The second special case, called the quasi-steady approximation, arises when diffusion is very rapid in comparison to reaction. This situation occurs frequently in applications such as silicon oxidation and provides a useful comparison test case for numerical methods.

In the present study, we consider mass transport with reaction at a boundary, for a representative class of one-dimensional problems. A finite element method is developed for the numerical solution of the model problem with the aim of predicting the location of the moving interface as the reaction proceeds in time. Thus, the problem is intrinsically a transient one, and moving finite elements provide a promising approach because the mesh can be easily made to fit the boundary configuration and allowed to stretch in response to boundary motion. Numerical studies are used to ascertain the effect of diffusion and reaction on the boundary motion and transport process. Time-step refinement studies are performed to determine the sensitivity of the method to the choice of time step and accurately determine the solutions. Comparison studies with an analytic solution for the quasi-steady case are used to assess numerically the accuracy and stability of the method.

The Model Problem

Governing Equations

Consider an isothermal chemical reaction $A + B \rightarrow C$ in which species A diffuses through the layer of product C to react at the surface of reactant B (see Fig. 1). Component B is impervious to the diffusing species and is converted to product C in the reaction. At the "free" surface of C, the concentration of A is known; at the interface between B and C, the mass flux of A is equal to the reaction rate which is a function of the concentration of species A.

We seek to model the transport of species A through the product layer and the movement of the reacting boundary. The associated mathematical model for this process consists of two coupled time-dependent differential equations. First, there is the diffusion equation for species A with reaction at a boundary $x = s(t)$

$$\frac{\partial u}{\partial t} - \mathscr{D}\frac{\partial^2 u}{\partial x^2} = 0 \qquad 0 < x < s(t),\ 0 < t \leqq T \tag{1}$$

$$u(0, t) = f(t) \qquad 0 \leqq t \leqq T \tag{2}$$

$$-\mathscr{D}\frac{\partial u}{\partial x}(s(t), t) = k\, r(u(s(t), t)) \qquad 0 < t \leqq T \tag{3}$$

$$u(x, 0) = \phi(x) \qquad 0 \leqq x \leqq b = s(0) \tag{4}$$

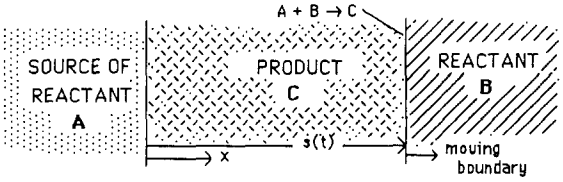

FIG. 1. Reaction at a boundary.

and, second, a nonlinear ordinary differential equation characterizing the motion of the boundary

$$N\dot{s}(t) = k\, r(u(s(t), t)) \qquad 0 \leqq t \leqq T \tag{5}$$

$$s(0) = b, \tag{6}$$

where $u(x, t)$ is the concentration of species A, $\mathscr{D}$ is the diffusivity, k is the reaction rate coefficient, N is the mass of reaction, $f(t)$ is a prescribed interface concentration, $\phi(x)$ is the initial concentration, and $s(t)$ is the position of the moving boundary. The domain in (x, t) space is illustrated in Fig. 2. Both equations are coupled together through the unknown boundary position $s(t)$. For reaction rate $r(u) = u$, the boundary condition (3) is linear and the reaction is first order; $r(u) = u^2$ corresponds to a second-order reaction and a nonlinear boundary condition. The solution is given by the pair (u, s) satisfying (1), (5) together with boundary conditions (2), (3) and initial conditions (4), (6).

Variational Problem

There are several ways in which a variational statement of the problem may be constructed. The approach we consider is quite straightforward and easily utilized in a finite element analysis. Let $\Omega(t)$ be the spatial domain $0 \leqq x \leqq s(t)$ at any time t. Integrating by parts the weighted integral of (1) on $\Omega(t)$, we obtain

$$\int_{\Omega(t)} (u_t v + \mathscr{D} u_x v_x)\, dx - \mathscr{D} u_x v \Big|_0^{s(t)} = 0, \tag{7}$$

where v is the test function (weight function).

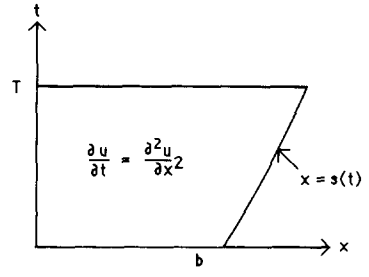

FIG. 2. Domain for the model problem in (x, t) space.

Using (2) and (3), $v(0)=0$ and $-\mathscr{D}u_x = k\,r(u)$ at $x=s(t)$. Then from (7) the variational problem is to find $u(x, t)$ satisfying the initial data and essential boundary condition, such that

$$\int_{\Omega(t)} (u_t v + \mathscr{D}u_x v_x)\,dx + k\,r(u(s(t), t))\,v(s(t)) = 0 \tag{8}$$

for all admissible test functions v. Here, $s(t)$ is not known *a priori* but is to be determined concurrently as the solution of (5), (6); that is, of

$$N\dot{s} = k\,r(u(s(t), t)), \qquad s(0) = b. \tag{9}$$

Transformation techniques may be applied to accommodate the moving boundary effect and to adjust the finite element mesh adaptively in the following approximate analysis as in Mueller and Carey (8). Introducing the transformation $x = x(\xi, \tau)$, $t = \tau$, the time derivative becomes, on using the chain rule, inverse map, and transposing,

$$\frac{\partial u}{\partial t} = \frac{\partial u}{\partial \tau} + \frac{\partial u}{\partial \xi}\frac{\partial \xi}{\partial t} = \frac{\partial u}{\partial \tau} - \frac{\partial u}{\partial x}\frac{\partial x}{\partial \tau} = \frac{\partial u}{\partial \tau} - V\frac{\partial u}{\partial x}, \tag{10}$$

where $V(x, \tau) = \partial x/\partial \tau$ is the velocity of point (x, τ) in the domain $\Omega(\tau)$. Thus, the effect of the transformation is to introduce the addition convective term $-V(\partial u/\partial x)$ in the differential operator to account for the domain deformation. In the present case, the boundary motion is specified as the solution of (9) with $V(s(\tau), \tau) = \dot{s}$ and we allow points in the interior to move proportionally so that $V(x, \tau) = (x/s)\,\dot{s}$ (e.g., see Lynch [7]).

Substituting (10) in (8), the transformed variational integral is

$$\int_{\Omega(\tau)} (u_\tau v - V u_x v + \mathscr{D}u_x v_x)\,dx + k r(u(s(\tau), \tau))\,v(s(\tau)) = 0, \tag{11}$$

where $s(t)$ is related to u by (9).

Approximate Formulation

Let $\Omega_h(\tau)$ denote the finite element discretization of the domain and $\{\psi_j\}$ the finite element basis so that the finite element expansion has the form

$$u_h(x, \tau) = \sum_{j=1}^{n} u_j(\tau)\ \psi_j(x). \tag{12}$$

Setting u_h in (12) for u and $v_h = \psi_i$ for v in (11) yields the semidiscrete system of ordinary differential equations

$$\mathbf{M}\dot{\mathbf{u}} - \mathbf{C}\mathbf{u} + \mathbf{A}\mathbf{u} + \mathbf{q}(\mathbf{u}) = \mathbf{0} \tag{13}$$

$$\dot{s} = \frac{k}{N} r(u_n), \qquad u_n(\tau) = u(s(\tau), \tau), \tag{14}$$

where $\mathbf{C}$ depends on $V(x, \tau)$ and $q_i = k\, r(u_n)\, \delta_{in}$, Kronecker delta δ_{in}.

In the solution algorithm, we have adopted the strategy of iteratively separating the calculation of $\mathbf{u}$, s, and V. Initially, $\mathbf{u}$, s, and hence V are known. Using this initial value of V, assumed constant through the first time step, the system (13)–(14) may be solved iteratively. To integrate (13)–(14), we have chosen backward differencing of $\dot{\mathbf{u}}$ and either forward or midpoint differencing of $\dot{s}$. An iterative uncoupling of the two equations is achieved by lagging the nonlinear term in (14) one time step and predicting the moving boundary position s at time $t + \Delta t$ using information about $\mathbf{u}$ at time t; V is updated using $\mathbf{u}$ at the end of the step. A more sophisticated method would be to retain a stronger coupling by alternately predicing and correcting for s. These predictor–corrector integration methods and the associated linearized equations are explained in more detail during the discussion of numerical results.

Nondimensionalization and the Quasi-Steady Case

Introducing the dimensionless quantities

$$u^* = \frac{u}{\bar{u}}, \qquad x^* = \frac{x}{l}, \qquad t^* = \frac{t}{\bar{t}}, \qquad s^* = \frac{s}{l},$$

the nondimensional form of (1)–(6) becomes (dropping the asterisk)

$$\alpha \frac{\partial u}{\partial t} - \frac{\partial^2 u}{\partial x^2} = 0, \qquad 0 < x < s(t),\ 0 < t \leqq T \tag{15}$$

$$u(0, t) = \hat{f}(t) \qquad 0 \leqq t \leqq T \tag{16}$$

$$-\frac{\partial u}{\partial x}(s(t), t) = \mathrm{Bi}\, r(u(s(t), t)) = \beta\, \dot{s}(t) \qquad 0 < t \leqq T \tag{17}$$

$$u(x, 0) = \hat{\phi}(x) \qquad 0 \leqq x \leqq b, \tag{18}$$

where $\alpha = l^2/\mathscr{D}\tau$, the Biot number $\mathrm{Bi} = kl/\mathscr{D}$, $\beta = Nl^2/\bar{u}\mathscr{D}\bar{t}$, $\hat{f} = f/\bar{u}$, and $\hat{\phi} = \phi/\bar{u}$. The quantities l, $\bar{t}$, and $\bar{u}$ denote characteristic length, time, and concentration, respectively. Note that for a first-order reaction $r(u) = u$, if $\mathrm{Bi} \to \infty$ the reaction condition $-\partial u/\partial x = \mathrm{Bi}\, u$ can be replaced by the condition $u = 0$ at $x = s(t)$, yielding the classical Stefan problem.

When diffusion is very rapid in comparison to reaction, transient delay is negligible in the diffusion process. The concentration $u(x, t)$ still remains a time-dependent function, but only on account of the changing domain. During a small time increment δt as the boundary advances from $s(t)$ to $s(t + \delta t)$, the concentration

distribution essentially adjusts itself instantaneously to the new domain without any transient delay. Mathematically, this condition is achieved in the limit as $\alpha \to 0$ with $\mathrm{Bi}/\beta < \infty$. For this quasi-steady case, the nondimensional equations (15)–(18) become

$$\frac{\partial^2 u}{\partial x^2} = 0 \qquad 0 < x < s(t),\ 0 < t \leqq T \tag{19}$$

$$u(0, t) = \hat{f}(t) \qquad 0 \leqq t \leqq T \tag{20}$$

$$-\frac{\partial u}{\partial x}(s(t), t) = \mathrm{Bi}\, r(u(s(t), t)) = \beta \dot{s}(t) \qquad 0 < t \leqq T \tag{21}$$

$$u(x, 0) = \hat{\phi}(x) \qquad 0 \leqq x \leqq b. \tag{22}$$

The analytic solution for (19)–(22) in the case of a first-order reaction $r(u) = u$ and $\hat{f}(t)$ constant, say $\hat{f} = 1$, is

$$u(x, t) = 1 - \frac{\mathrm{Bi}}{1 + \mathrm{Bi}\, s(t)} x \tag{23}$$

$$s(t) = \frac{1}{\mathrm{Bi}} \left[\sqrt{1 + 2\,\mathrm{Bi}((\mathrm{Bi}/\beta)\, t + b + \tfrac{1}{2}\,\mathrm{Bi}\, b^2)} - 1\right]. \tag{24}$$

The large and short time asymptotic behavior of $s(t)$ is of particular interest and can be easily deduced from (24): For large time ($t \gg \beta/2\mathrm{Bi}^2$)

$$s(t) \propto \sqrt{(2/\beta)\, t}, \tag{25}$$

whereas, for small times ($t \ll \beta/2\mathrm{Bi}^2$),

$$s(t) \propto \frac{\mathrm{Bi}}{\beta} t + b + \frac{1}{2}\,\mathrm{Bi}\, b^2. \tag{26}$$

Note that $\dot{s} \to 0$ and $s \to \infty$ as $t \to \infty$. In the chemical engineering literature, the quantities $(2/\beta)(l^2/\bar{t})$ and $(\mathrm{Bi}/\beta)(l/\bar{t})$ are called the parabolic and linear rate constants, since they determine the respective asymptotic square root and linear growth rate of $s(t)$.

Numerical Studies

Solution Methods

Numerical studies are performed on the model problem (15)–(18) with $r(u) = u$, $\hat{f}(t) = 1$, $\hat{\phi}(x) = 0$, and $b = 1$. An accurate spatial approximation of u is achieved by using 10 quadratic elements on the interval $x = 0$ to $x = s(t)$. The resulting semi-discrete system given by (13)–(14) is integrated from $t = 0$ to $t = T$; time evolution of

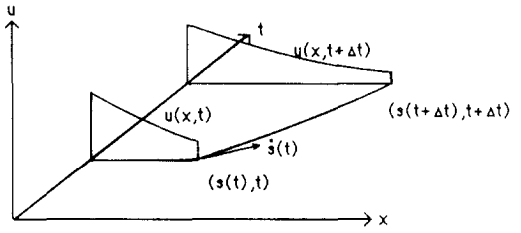

FIG. 3. Time evolution of $(u(x, t), s(t))$ through an interval Δt.

the solution (u, s) through a time step Δt is schematically illustrated in Fig. 3. Computational experience shows that overall accuracy in one-dimensional problems is limited by the accuracy of time integration; therefore, we focus on this aspect of the approximation. The integration of $\dot{\mathbf{u}}$ and $\dot{s}$ are coupled through the reaction rate term in (14) which is implicitly a function of $\mathbf{u}$ and s. We iteratively uncouple the equations by alternately solving (13) and (14) where $u(s(t), t)$ in (14) is determined from a prior solution of (13). An implicit method (backward differencing) for the integration of (13) is used because explicit methods place too stringent a stability restriction on the time step—much more than that required for the integration of (14).

A predictor and a predictor–corrector method are used to integrate (14) and their performance compared. The predictor method is given by

$$s_p^{n+1} = s^n + \Delta t \frac{k}{N} r(u^n(s^n)), \tag{27}$$

where the superscripts denote the time level and Δt the time step size. This method utilizes information about u at time t to predict the boundary position at time $t + \Delta t$ and is therefore explicit. Alternatively, we can use information about both u^n and u^{n+1} to compute s^{n+1}. One such approach is a predictor–corrector method

$$s_c^{n+1} = s^n + \Delta t \dot{s}^{n+1/2}, \tag{28}$$

where $\dot{s}^{n+1/2}$ is a midpoint approximation to the boundary velocity given by

$$\dot{s}^{n+1/2} = \tfrac{1}{2}(\dot{s}^n + \dot{s}_p^{n+1}). \tag{29}$$

A predicted position s_p^{n+1} is first computed from (27), then (28)–(29) applied to yield the corrected position given by

$$s_c^{n+1} = s^n + \frac{\Delta t}{2} \frac{k}{N} [r((u^n(s^n)) + r(u^{n+1}(s_p^{n+1}))]. \tag{30}$$

This algorithm is illustrated schematically in Fig. 4. Note that $u^{n+1}(s_p^{n+1})$ appears in (30), requiring an integration of $\dot{u}$ in advancing from s^n to s_p^{n+1}. When a correc-

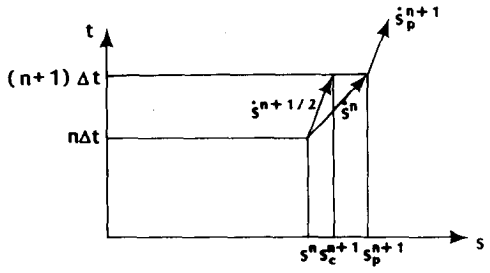

FIG. 4. Predictor–Corrector method for advancing the boundary.

ted position s_c^{n+1} has been determined, a new integration of $\dot{u}$ is then performed from s^n to s_c^{n+1}. With $u^{n+1}(s^{n+1})$ now obtained, the predictor–corrector process is repeated for the next time step.

Given a computed $\dot{s}$, whether at a predictor or corrector step, a stretching transformation advances all other nodes inside the domain by an amount proportional to their distance from the moving boundary. Nodal velocities are then used in the calculation of the convection matrix **C** in (13) to account for a changing domain through the time step.

Parametric Studies

In the numerical studies, we experiment with the predictor and predictor–corrector methods for integration of $\dot{s}(t)$, ascertain the sensitivity of the method to the choice of time step, verify accuracy by comparison with the quasi-steady analytic solution, and assess the influence of variations in α, Bi, and β on the motion of the boundary.

In the model problem (15)–(18) with a first-order reaction, data was taken to be $\hat{f}=1$, $b=1$, and $\hat{\phi}=0$. To approximate closely the quasi-steady case, nondimensional parameters were chosen as $\alpha=0.001$, $\mathrm{Bi}=1$, and $\beta=1$. Convergence to the quasi-steady analytic solution with time step refinement is shown in Fig. 5, in which the boundary position $s(t)$ is plotted as a function of time. Integration of $\dot{s}$ was performed by the predictor method. The boundary concentration $u(s(t), t)$ is plotted as a function of time in Fig. 6 for the same set of data. It is seen that large time steps produce significant errors in the boundary concentration for short times which eventually diminish with $u(s) \to 0$ as $t \to \infty$. However, the initial errors in $u(s(t), t)$, being proportional to $\dot{s}(t)$, cause significant errors in the computation of $s(t)$ that remain through time. Therefore, accurate time integration throughout is required even if the solution is desired only at some large time.

A comparison was made between the predictor and predictor–corrector methods again for the case $\alpha=0.001$, $\mathrm{Bi}=1$, and $\beta=1$. Convergence to the quasi-steady solution for $s(t)$ is illustrated in Fig. 7, and indicates that much larger time steps can be taken with the predictor–corrector method versus the predictor method to

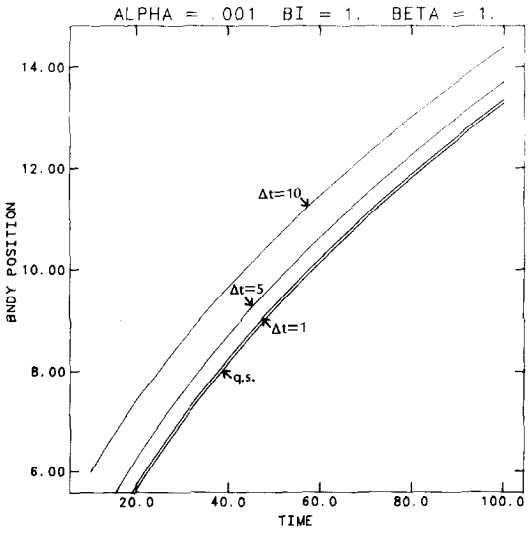

FIG. 5. Convergence of computed boundary position to the quasi-steady solution with time-step refinement (predictor method).

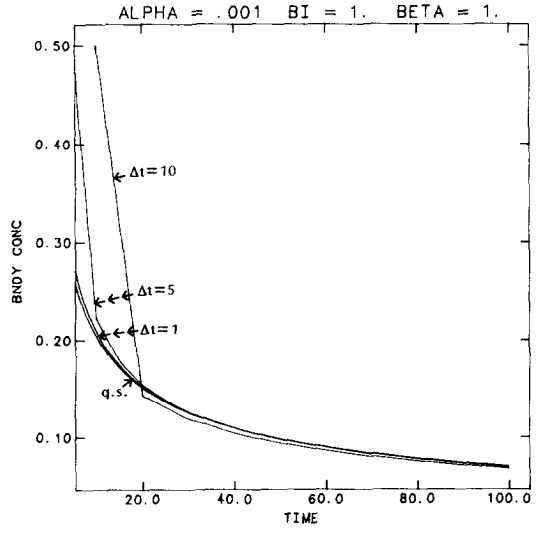

FIG. 6. Convergence of computed boundary concentration to the quasi-steady solution with time-step refinement (predictor method).

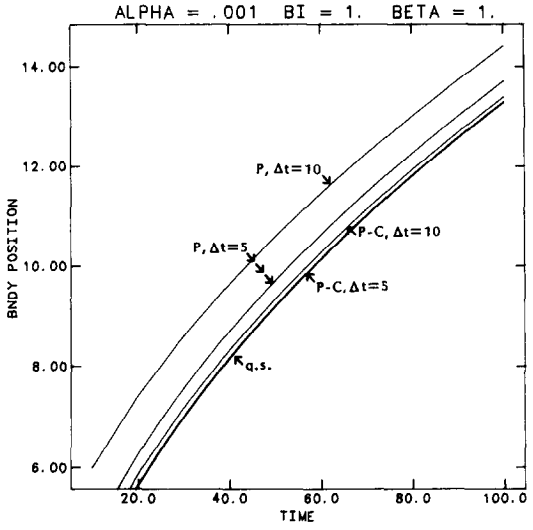

FIG. 7. Comparison of predictor (P) and predictor–Corrector (P–C) method for convergence of computed boundary position to the quasi-steady solution.

achieve equivalent accuracy. However, more computational effort per step is required and this must also be considered when choosing an integration method.

To assess the convergence and stability of the predictor method for the time-dependent model problem, the effect of time-step refinement on the computed boundary position $s(t)$ and concentration $u(s(t), t)$ is evaluated. The parameters in

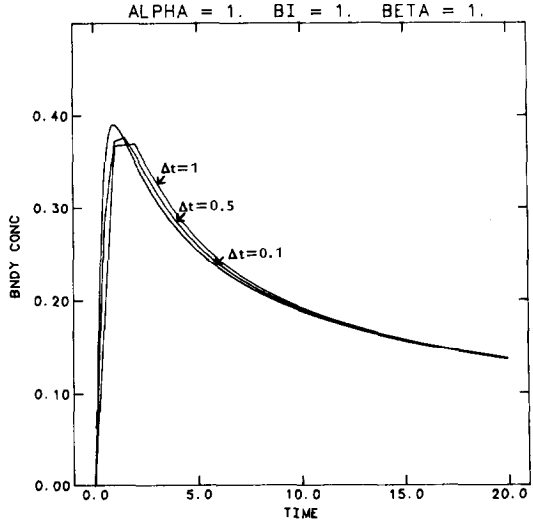

FIG. 8. Effect of time-step refinement on computed boundary concentration.

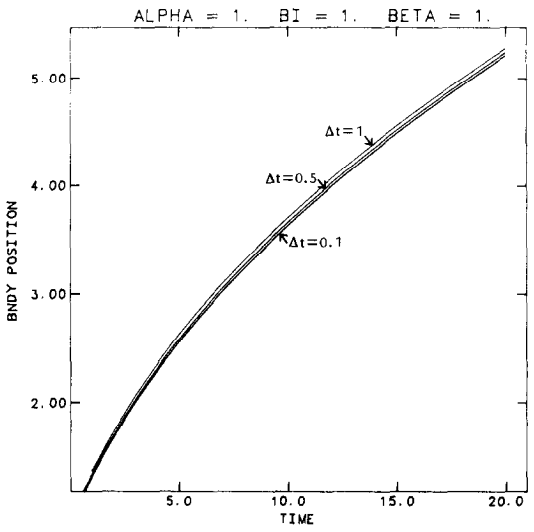

FIG. 9. Effect of time-step refinement on computed boundary position.

the model are now chosen as $\alpha = 1$, $\mathrm{Bi} = 1$, and $\beta = 1$, which produce appreciable changes in $u(s(t), t)$ and hence, changes in $\dot{s}(t)$, over the time of integration. For an initial concentration of zero, the differential equation for $s(t)$ is stiff for short times during which the boundary concentration rapidly increases until it begins slowly depleting due to reaction (see Fig. 8). The diffusion process wants to raise the concentration to a steady state value, while the reaction process seeks to deplete mass through reaction at the boundary. The combined effect of the two processes with widely different time scales produces a stiff region for short times, necessitating the use of very small time steps for acceptable accuracy (see Fig. 8).

For the range of time steps considered, all solutions are stable in the sense that the computed boundary position is neither diverging from the exact position nor oscillating between overshoot and undershoot. (The latter situation is frequently encountered in numerical approximation of Stefan problems.) Using a predictor to integrate $\dot{s}(t)$ would tend to overshoot the exact boundary position and, as the computations show, remain that way. Applying a corrector tends to reduce the amount of overshoot since the resulting midpoint approximation of $\dot{s}(t)$ is more accurate than the forward-Euler approximation of the predictor. On the basis of physical reasoning, if the computed boundary position is larger than the exact position, the resulting velocity decrease ($\dot{s} \to 0$ as $t \to \infty$) would tend to prevent instability by slowing down a boundary advancing too rapidly.

The effect of variations in α, Bi, and β on $s(t)$ is illustrated in Figs. 10–12. Decreasing α toward zero while holding Bi and β constant (Fig. 10) approaches the quasi-steady situation. If instead, *Bi* is increased while holding α and β constant (Fig. 11), we approach a diffusion-controlled situation in which the motion of $s(t)$ is

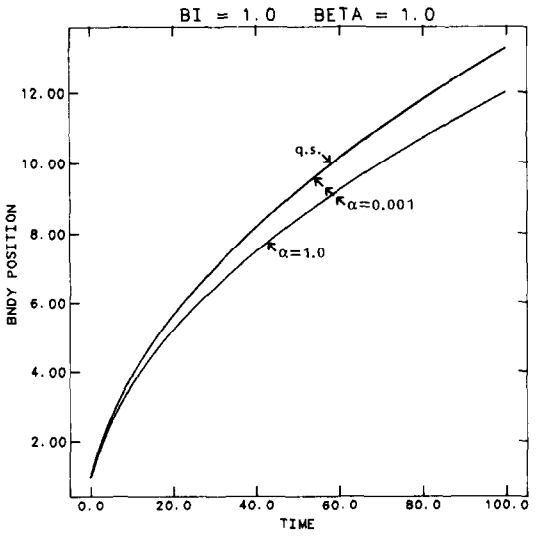

FIG. 10. Effect of variations in α on computed boundary position.

limited by the amount of mass reaching the boundary. The concentration $u(s(t), t)$ is nearly zero in this situation. Further increasing Bi results in negligible change in $s(t)$ since most of the mass at the boundary has been depleted, leaving little additional mass for an increased reaction. Finally, increasing β while holding α and Bi constant (see Fig. 12) slows down the motion of the boundary. Hence, the limiting situation of $\beta \to \infty$ degenerates to $\dot{s}(t) = 0$, or no boundary motion.

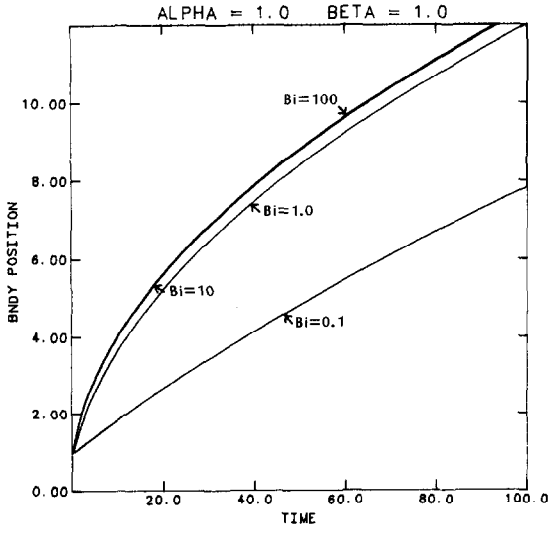

FIG. 11. Effect of variations in Bi on computed boundary position.

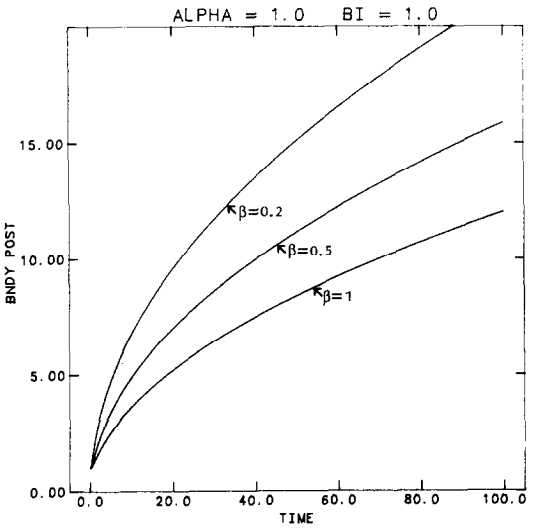

FIG. 12. Effect of variations in β on computed boundary position.

We have discussed above the quasi-steady case ($\alpha = 0$) and compared the associated analytic solution with numerical results obtained for α small. In fact, for $\alpha = \varepsilon$, $0 < \varepsilon \ll 1$ a regular perturbation analysis may be introduced to obtain an asymptotic expansion for u and s in ε. In this analysis, the problem domain is first transformed to a fixed domain by the time-dependent transformation $\xi = x/s(t)$ and the perturbation expansions for u and s introduced in the transformed problem. The formal analysis is similar to that in Carey and Murray [3] for the analogous problem in spherical geometry called the "shrinking core" model. Matching terms to first order in ε, the two-term perturbation approximation to the boundary position is, for the case $\mathrm{Bi} = 1$, $\beta = 1$, $\hat{f} = 1$, and $b = 0$,

$$s(t) = s_0(t) + \varepsilon s_1(t), \tag{31}$$

TABLE I

Comparison of Finite Element and Perturbation Solutions of $s(t)$ at $t = 20$ for Various Values of the Perturbation Parameter ($\mathrm{Bi} = 1$, $\beta = 1$, $s(0) = 0$)

	Perturbation Parameter		
	0.1	0.5	1.0
Perturbation solution	5.35877	5.18135	4.95958
Finite element solution	5.35995	5.20483	5.04239
Quasi-steady approximation	5.40312	5.40312	5.40312

where $s_0(t)$ is the quasi-steady solution

$$s_0(t) = \sqrt{1+2t} - 1 \tag{32}$$

and $s_1(t)$ is the solution of

$$(1+s_0)^3 \dot{s}_1 + (1+s_0)\, s_1 + \tfrac{1}{3} s_0^3 \dot{s}_0 = 0, \qquad s_1(0) = 0 \tag{33}$$

and is evaluated numerically. Results for the quasi-steady solution, perturbation solution and finite element solution are compared in Table I for several values of ε. The perturbation solution provides valid results for ε sufficiently small, but the finite element analysis is quite generally applicable and may, of course, be extended to include the case of a nonlinear reaction as indicated next.

Consider the model problem (15)–(18) with a second-order reaction rate $r(u) = u^2$. The contribution of this boundary condition to the approximate formulation ($\mathbf{q}(\mathbf{u})$ in (13)) is nonlinear and the resulting nonlinear algebraic equations may be solved by the method of successive substitution. To do this, we approximate the boundary condition as

$$q_n^{i+1} = k\, r(u_n) \doteq k\, u_n^i u_n^{i+1}, \tag{33}$$

where i denotes the iteration number in the successive substitution method. Iteration continues until the difference between successive iterates of u_n is less than a specified tolerance.

Computational results for the second-order rate equation may be compared with those obtained using a first-order rate for the parameters $\alpha = 1$, $Bi = 1$, $\beta = 1$, $\hat{f} = 1$,

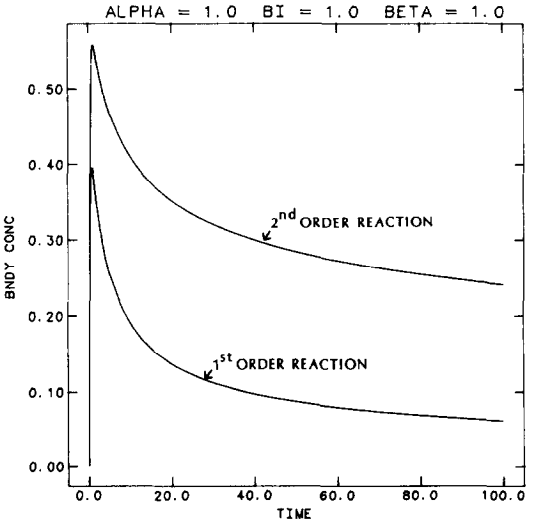

FIG. 13. Computed boundary concentration for first- and second-order reaction rates.

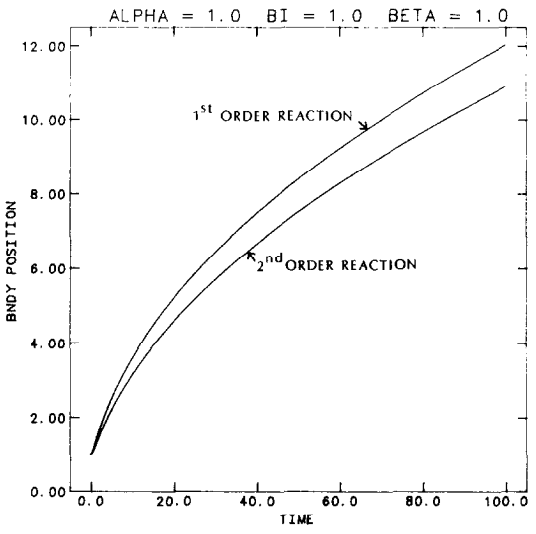

FIG. 14. Computed boundary position for first- and second-order reaction rates.

$\hat{\phi} = 0$, and $b = 1$ and some interesting points emerge. A tolerance of 0.1% is used for the nonlinear iteration and convergence obtained in one to three iterations per time step. In particular, we observe that the concentration at boundary $x = s(t)$ (Fig. 13) for the second-order reaction is higher than that for the first-order reaction. This implies that more mass is available for the reaction. However, since the boundary velocity is proportional to the square of the concentration,

$$\dot{s}(t) = \frac{Bi}{\beta} u(s(t), t)^2$$

and $u(s(t), t) < 1$, so it is plausible that the rate of chemical conversion is less than that obtained with a first-order reaction. This has been verified in the numerical results (Fig. 14); thus, the domain grows more slowly for this particular nonlinear reaction.

CONCLUDING REMARKS

We have considered the problem of diffusion with reaction at a moving boundary and developed a finite element method employing a moving mesh and iterative linearization of the coupled nonlinear system of equations. Computations performed in one dimension illustrate the effectiveness of the method and uncover important physical aspects of the solution behavior related to the effects of diffusion and reaction. The quasi-steady case is examined because of its importance in many

physical phenomena and the fact that it admits a simple analytic solution. This solution is included and used in the supporting verification studies for the approximate method and solution procedure.

Often, the medium through which diffusion occurs is a fluid and, in two-dimensional problems, may be in motion due to volume expansion, buoyancy, forced convection, or other effects. The problem then becomes a coupled fluid flow and transport problem with reaction at a boundary. We are presently investigating this case for reaction at a fixed boundary [9]; future studies will be directed toward the solution of two-dimensional coupled problems with reaction at a moving boundary.

ACKNOWLEDGMENT

This research has been supported in part by the Office of Naval Research.

REFERENCES

1. R. B. BIRD, W. E. STEWART, AND E. N. LIGHTFOOT, Transport Phenomena (Wiley, New York, 1960).
2. J. R. CANNON, The One-Dimensional Heat Equation (Addison–Wesley, Reading, MA, 1984).
3. G. F. CAREY AND P. MURRAY, *Chem. Eng. Sci.*, in review.
4. B. E. DEAL AND A. S. GROVE, *J. Appl. Phys.* **36**, 3770 (1965).
5. A. FRIEDMAN, Variational Principles and Free Boundary Problems (Wiley, New York, 1982).
6. I. GLASSMAN, Combustion (Academic Press, New York, 1977).
7. D. R. LYNCH, *J. Comput. Phys.* **47**, 387 (1982).
8. A. MUELLER AND G. F. CAREY, *Int. J. Num. Meth. Eng.* **21**, 2099 (1985).
9. P. MURRAY AND G. F. CAREY, *Chem. Eng. Sci.*, in press.